REDUCTION OF OXYGEN TO PEROXIDE IN A TRICKLE ELECTRODE

Otomar ŠPALEK and Karel BALOGH

Institute of Inorganic Chemistry, Czechoslovak Academy of Sciences, 160 00 Prague 6

Received August 18, 1988
Accepted October 24, 1988

The effects of the electrode material particle size, electrode thickness, diaphragm properties and gas and electrolyte flow rates on the pressure loss and liquid holdup in the electrode and on the current efficiency of peroxide formation by oxygen reduction were studied in a trickle electrode. The results are discussed using trickle-bed electrode calculations.

On catalytically low-active carbon electrodes, oxygen is reduced giving hydrogen peroxide or, in alkaline solutions, perhydroxyl ions:

$$O_2 + H_2O + 2\,e \rightarrow OH^- + HO_2^- . \qquad (A)$$

Reduction of perhydroxyl ions

$$HO_2^- + H_2O + 2\,e \rightarrow 3\,OH^- \qquad (B)$$

proceeds at a relatively high overvoltage, so that within a suitable potential region, oxygen can be reduced selectively at such electrodes to produce peroxide.

A factor limiting the rate of this process is the low concentration of reactant, i.e. oxygen dissolved in the electrolyte; due to this, reduction current densities are very low at smooth electrodes. Technologically feasible current densities can only be achieved using large surface area electrodes. This concept of electrochemical synthesis of peroxide dates rather far back[1], but although several research teams have concerned themselves with it, this process has not as yet found application on an industrial scale.

Earlier research was oriented particularly to the use of gas diffusion electrodes[1-5]; laboratory preparation of electrodes with several thousand hours service life was mastered. These electrodes can be employed to prepare alkaline solutions containing 0·5–0·8 mol peroxide per mol KOH (refs[3,5]) or NaOH (refs[5,6]) at current densities of 0·5–2 kA m^{-2} and peroxide current efficiencies 70–90%.

Gas diffusion electrodes large enough for industrial application, however, suffer from some imperfections such as insufficient mechanical resistance and limited service life caused by the negative effect of hydrostatic pressure of electrolyte. In

view of this, the activity of several research teams in the world has been concentrated in the last decade on developing another type of large surface-area electrodes for this process, namely, trickle-bed electrodes[7-14].

The first to study this system, most extensively so far, were Oloman and Watkinson[7-9], who found that when using trickle-bed electrodes of crushed graphite, peroxide can be prepared at technologically reasonable current densities of 0·5 to 1·5 kA m^{-2} and current efficiencies of 60–80% only if elevated pressures of 0·9 to 2·2 MPa are applied. The peroxide concentrations in the outgoing solutions, 0·1 to 0·5 mol per mol hydroxide, were lower than as attained with gas diffusion electrodes. An appreciable asset of this approach as compared to the use of gas diffusion electrodes lies in the possibility of employing sodium electrolytes without cathode breakdown hazard.

The electrode potential of a trickle-bed electrode as well as the peroxide yield are dependent on a number of factors such as the catalytic properties of the electrode material, its conductivity, wettability, particle size, electrode thickness, gas and electrolyte flow rates, current density, diaphragm transport properties, etc. To account for the effect of these factors, a mathematical model of the trickle electrode has been devised[13], allowing us, based on kinetic data of the reactions involved and on transport data, to estimate the loss of peroxide caused by its reduction, decomposition and transport through the diaphragm into the anode chamber.

This paper presents experimental results of basic measurements of the preparation of peroxide at crushed graphite electrodes and results of auxiliary measurements serving to characterize the trickle electrodes used.

EXPERIMENTAL

Trickle electrodes were prepared by pouring crushed graphite between a stainless steel plate current collector (1 in Fig. 1) and a PVC diaphragm or ionex membrane 2. In the measurements, S 42 type carbon-graphite (Elektrokarbon Topoľčany) was used. The anode was a nickel-plated stainless steel plate 3, at which oxygen was evolved. The cathodic section was sealed by

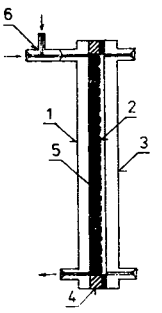

FIG. 1
Layout of electrolyzer containing a trickle-bed electrode. Description given in the text

means of a gasket 4 compressed between the cathode and anode plates. The trickle-bed electrode 5 height was 0·5 m, breadth 45 mm or 21 mm and thickness 2·3—5·5 mm. Electrolyte solution, viz. 2M-NaOH, and oxygen gas were mixed in injector 6. The mixture entered the trickle-bed electrode at its top and left it at its bottommost site. In the diaphragm-containing cell the anode chamber was not flow-through; the electrolyte ions reached the anode by transport through the diaphragm only. When the ionex membrane was employed, the electrolyte solution was fed to the anode chamber bottom and the mixture of the liquid with evolved oxygen left the anode chamber at its top, wherefrom it was brought to the injector. The gas-electrolyte mixture leaving the trickle electrode was fed to a stainless steel reduction valve and a phase separator. Hydrogen peroxide in the outgoing electrolyte was determined titrimetrically with permanganate. The electrolyte temperature at the outlet depended on the electrolyte flow rate and electrolysis current and voltage. For instance, at total currents of 10 and 20 A the electrolyte temperature was 10—20 and 30—35°C, respectively, above the ambient level (about 22°C).

Oxygen reduction measurements were usually performed at an oxygen flow rate of 35 $dm^3\ h^{-1}$ and electrolyte flow rates of 0·075, 0·15 and 0·3 $dm^3\ h^{-1}$; these data apply to the electrode breadth of 21 mm, for the broader electrode the flow rates were twice as high.

The temporary liquid holdup in the electrode was determined by measuring the volume of liquid leaving the trickle bed in 10 min after discontinuing the current and electrolyte supply while maintaining the oxygen feed uninterrupted.

The permanent liquid holdup was determined from the difference between the mass of the wet electrode material after finishing the temporary holdup measurement and the mass of this material after its washing and drying at 105°C. The liquid pore fraction was calculated from the liquid holdup volume and the total electrode porosity.

Porosity of the diphragm used was determined from the difference between the mass of the water-soaked diaphragm (after previous evacuation) and the mass of the dry diaphragm. The pore curvature coefficient was evaluated based on the effective electric resistance of the diaphragm. This resistance was measured in a cell with a variable distance of platinum-platinum black electrodes. The specific resistivities of the diaphragm ϱ_d and free electrolyte ϱ_e were evaluated from the experimental dependence of the cell impedance on the electrode distance in the absence and in the presence of the diaphragm. The pore curvature coefficient was calculated as

$$f_d = V_d(\varrho_d/\varrho_e)\,. \qquad (I)$$

The diaphragm permeability was evaluated by measuring the flow rate of water at a constant pressure difference at the diaphragm (6 kPa).

The kinetics of peroxide decomposition at the graphite surface was measured by two methods. In the first, 0·3 g of the graphite material was stirred in a flask containing 100 ml of 2M-NaOH + 1M-H_2O_2; in the other method, this solution was allowed to flow at a rate of 60 $cm^3\ h^{-1}$ through a crushed graphite bed 45 mm broad, 2·4 mm thick and 0·5 m long, and the peroxide concentration was determined after one passage through the bed. In both cases the peroxide concentration was determined permanganometrically. When calculating the decomposition at the graphite surface, the peroxide decomposition rates in the solution bulk and at the vessel walls were taken into account.

RESULTS AND DISCUSSION

Since reduction of oxygen in a trickle-bed electrode is controlled to a high extent by its transport, the pressure loss in the electrode is a significant parameter[13]. There-

fore, both single-phase pressure loss during the passage of oxygen, ΔP_G, and two-phase loss during the passage of oxygen and electrolyte (2M-NaOH), ΔP_{GL}, were measured in the electrodes used. The single-phase pressure loss in the beds under study were found to obey the equation suggested by Ergun for packed beds[15], viz.

$$\Delta P_G = (150 + 1{\cdot}75Re_G)\,\mu_G U_G(1 - \varepsilon)^2/(d'^2\varepsilon^3), \qquad (2)$$

where the particle diameter modified with respect to the bed size, d', is calculated as

$$d' = d/\{1 + (t + w)\,d/[3tw(1 - \varepsilon)]\}\,. \qquad (3)$$

The effective particle diameter, d, was calculated from the mean particle diameter and the particle roughness factor,

$$d = \bar{d}/f_p\,. \qquad (4)$$

The best fit of Eq. (2) data to pressure losses measured in the beds of crushed graphite was obtained using particle roughness factor values of 2 to 2·2. An example of dependences of the experimental and calculated losses on the gas flow rate is shown in Fig. 2. In experiments where one bed wall was a permeable diaphragm, the gas passed partly through this diaphragm and the anode chamber, so that the pressure losses decreased 1·2 to 12 times in dependence on the particle size and diaphragm permeability.

Two-phase pressure losses measured on passing oxygen and 2M-NaOH through the trickle-bed were fitted by the equation[16]

$$\Delta P_{GL} = \Delta P_L[1{\cdot}3 + 1{\cdot}85(\Delta P_L/\Delta P_G)^{-0{\cdot}425}]^2 \qquad (5)$$

The experimental values of ΔP_{GL} for crushed graphite bed separated from the anode

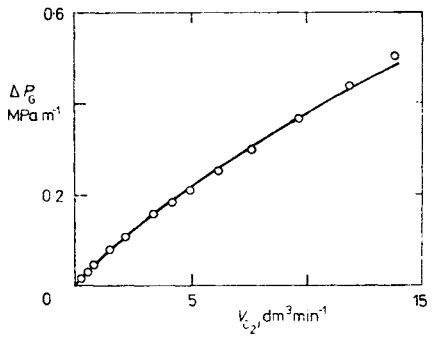

FIG. 2

Dependence of single-phase pressure loss in a bed of carbon-graphite 0·18—0·40 mm particle size on the oxygen flow rate. Bed dimensions 0·47 m (length), 45 mm (breadth), 3 mm (thickness), porosity 0·46, bed without diaphragm. Circles denote experimental values, curve corresponds to Eq. (2) for $f_p = 2{\cdot}1$

compartment by an impermeable membrane or in a diaphragm-less arrangement, were well fitted using particle roughness factors of 1·2–2·2 (Fig. 3).

Liquid holdup measurements were performed to determine the gas and liquid pore fractions in the trickle-bed electrode. The proportion of the pores filled by the electrolyte was calculated from the volume of liquid retained during electrode performance and the total electrode pore volume. Examples of dependences of temporary liquid holdup (pertaining to liquid leaving the electrode after the solution feed has been discontinued) on the gas and liquid flow rates are shown in Fig. 4. The curves in this figure are plots of the dependence

$$\beta_1 = 3{\cdot}86 Re_L^{0{\cdot}545} Ga^{-0{\cdot}42} (ad'/\varepsilon)^{0{\cdot}65} \qquad (6)$$

derived by Specchia and Baldi[17] based on measurements on non-electrochemical trickle beds with comparatively coarse particles (12 to 25 mm). Higher holdup values at higher pressures are due to the lower linear velocity of the gas in the electrode, associated with a lower pressure loss and a lower Galileo number value. As the gas flow rate is raised, both the single- and two-phase losses and the Galileo number increase and the liquid holdup decreases.

We found that in the electrodes studied, consisting of rather fine particles, a considerable amount of liquid sticks permanently to the graphite, as can be established

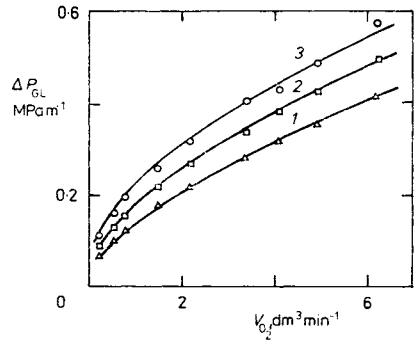

FIG. 3

Dependences of two-phase pressure loss in a bed as in Fig. 2 on the oxygen flow rate. Electrolyte flow rate (dm^3 h^{-1}): *1* 0·15, *2* 0·30, *3* 0·60. Curves correspond to Eq. (*5*) for $f_p = 1{\cdot}8$.

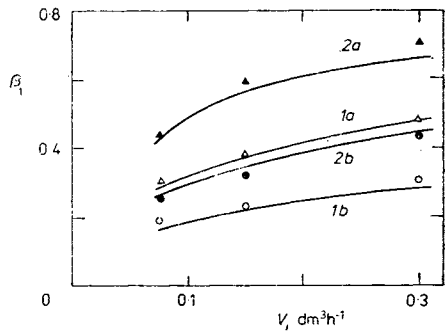

FIG. 4

Dependences of temporary holdup of 2M-NaOH in a trickle bed on the electrolyte flow rate. Bed dimensions 21 mm (breadth), 3 mm (thickness), porosity 0·46; Bären diaphragm. Exit overpressure (MPa): *1* 0, *2* 0·5. Oxygen flow rate (dm^3 min^{-1}): *1a*, *2a* 0·56, *1b*, *2b* 3·5. Curves correspond to Eq. (*6*) for $f_p = 1{\cdot}8$

by the procedure described in the Experimental. This holdup, referred to as permanent in this paper, was measured in crushed carbon-graphite beds with different particle sizes, using 2M-NaOH as electrolyte. The permanent holdup was considerable and increased from 0·25 for 0·63 – 1·0 mm particle size to 0·29 for 0·40 – 0·63 mm to 0·36 for 0·18 – 0·40 mm to 0·40 for 0·08 – 0·18 mm particle size. It is noteworthy, though, that some fraction of this liquid is not retained in the intergranular pores but in the inner pores of the graphite grains.

The basic properties of the diaphragms, viz. their porosity, electric resistance and permeability were also measured; an overview is given in Table I, where the V_p/f_p value is the ratio of the diffusion velocity in the diaphragm to the diffusion velocity in the free electrolyte.

The above results warrant the use of Eqs (*2*)–(*6*) for the calculation of pressure loss and temporary liquid holdup values in trickle-bed electrodes made of rather fine crushed graphite. Owing to this, these relations were employed in the mathematical model of a trickle-bed electrode using the above particle roughness factor values[13]. The established porosity and diaphragm pore curvature coefficient values were used for the calculation of the perhydroxyl ion losses by diffusion into the anode chamber.

The preparation of peroxide by cathodic reduction of oxygen was studied using electrodes made up from four crushed graphite fractions, grain size 0·08 – 0·18, 0·18 – 0·40, 0·40 – 0·63 and 0·63 – 1·00 mm. The dependences of the peroxide current efficiency and electrolysis voltage on the electrolyte flow rate and current density were measured; the current efficiency was found to decrease appreciably with current density (Fig. 5). The primary cause of this is in the increasing rate of peroxide reduction, which is the most significant loss process in a trickle bed[13]. According to calculations performed for the carbon-graphite electrode 0·18 – 0·40 mm particle size, peroxide losses due to reduction increase from 3 to 35% over the current density region of 140 – 880 A m^{-2} at an electrolyte flow rate of 0·6 dm^3 h^{-1}, losses by dif-

TABLE I

Thickness t_d, porosity V_d, pore curvature coefficient f_d and permeability P_d values of diaphragms used

Type	Material	t_d mm	V_d	f_d	$P_d \cdot 10^{16}$ m^2	V_d/f_d
Volpor	PVC	0·2	0·77	11·2	3·8	0·069
Bären	PVC	0·15	0·35	2·63	1 700	0·133
FS 2121	PP	0·2	0·78	2·11	65 000	0·37

fusion and migration into the anode chamber increase from 3·9 to 7%, whereas losses by decomposition decrease from 4·2 to 3·1% (all with respect to the total rate of peroxide formation). The lower peroxide yields at lower electrolyte flow rates are due to the higher concentration of peroxide in catholyte and the associated higher rates of all loss processes, i.e. peroxide reduction, decomposition and transport to the anode chamber. As the electrolyte flow rate is reduced, the pressure loss in the electrode decreases and so do the mass transport coefficients in the electrode, whose potential shifts to more negative values[13,18].

Peroxide concentration in the outflowing electrolyte increased with increasing current density; it attained 0·5, 0·34 and 0·24 mol dm^{-3} at the lowest, medium and highest flow rates, respectively. Electrolysis voltage increased nearly linearly with current density, from 1·4 to 2·3 V over the region of 220–880 A m^{-2}.

When using a coarser graphite fraction in the electrode (Fig. 6), the current efficiencies decrease more rapidly with increasing current density because of the limited oxygen transport rate – due to the lower mass transport coefficient values brought about by the lower pressure loss in this electrode and by its smaller surface area. According to calculations of this electrode for an electrolyte flow rate of 0·6 dm^3 .

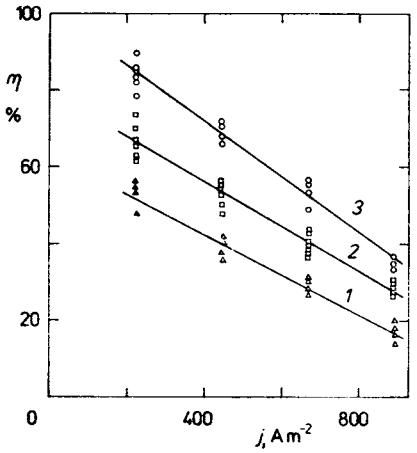

FIG. 5

Dependences of peroxide current efficiencies on current density for a carbon-graphite electrode 0·18–0·40 mm particle size, 0·47 m (length), 45 mm (breadth), 3·4 mm (thickness) bed dimensions. Exit overpressure 1 MPa, Bären diaphragm. Gas flow rate 0·56 dm^3 . . min^{-1}, electrolyte (2M-NaOH) flow rates (dm^3 h^{-1}): *1* 0·15, *2* 0·30, *3* 0·60

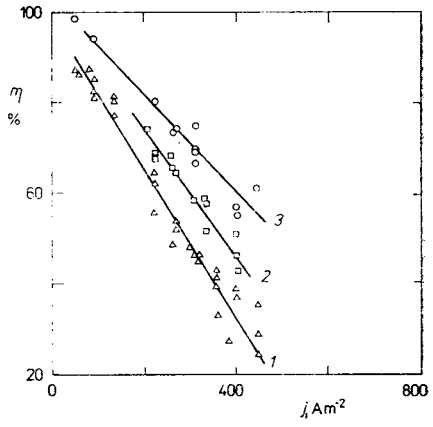

FIG. 6

Dependence of peroxide yield on current density for a carbon-graphite electrode 0·63–1·00 particle size. Labelling and description as in Fig. 5, Volpor diaphragm

. h^{-1}, peroxide losses by reduction increase from 3 as far as 50% over the current density region of 120–400 A m^{-2}; losses by decomposition are low (0·8–1·3%).

In electrodes containing a fine graphite fraction (0·08–0·18 mm) and using a Bären diaphragm, peroxide yields are very low, decreasing from 55 to 3% over the current density region of 100–450 A m^{-2}. As a matter of fact, theoretically the yields should be much higher, 75–85% over the region indicated, owing to the high mass transport coefficient values and large electrode surface area, which should bring about relatively positive potentials and low peroxide losses by reduction (4–8%). However, the experimental pressure losses in the electrolyzer with this electrode were 15 to 20 times lower than the calculated values; this indicates that with this electrode, exhibiting a high hydraulic resistance, a substantial fraction of the two phases passes through the diaphragm and the anode chamber, so that the oxygen transport in the electrode is reduced considerably. When a less permeable Volpor diaphragm was used, the pressure loss was 2 to 5 times higher and accordingly, peroxide current efficiency was as much as 20% higher than as attained with the Bären diaphragm.

Thus, the results indicate that the performance of a trickle-bed electrode is highly dependent upon the permeability of the diaphragm employed. Similarly, when measuring oxygen reduction in an electrode made of the medium graphite fraction (0·18–0·40 mm) and separated from the anode chamber by highly permeable polypropylene felt (Table I), peroxide yields are considerably (20–50%) lower than those shown in Fig. 5. It is noteworthy that the effect of the peroxide fraction permeating into the anode chamber by diffusion and migration is not so high in this arrangement; calculations give mere 12–17% as compared to the 4–7% for electrolysis with the Bären electrode (over the 140–880 A m^{-2} current density region and at an electrolyte flow rate of 0·6 dm^3 h^{-1}).

Experimentally found low current efficiency of peroxide in this arragement can hence be explained by the parallel gas and electrolyte flows through the anode compartment, which brings about high transport hindrances, negative potential and high peroxide loss by its reduction.

The highest peroxide yields are achieved if the electrode chambers are separated by an ionex membrane. In addition to elimination of peroxide losses by diffusion and migration into the anode chamber, the membrane ensures that all the gas and electrolyte pass through the porous cathode. The pressure loss then is higher than with the use of a diaphragm. Current efficiencies for the electrode made from the medium-size graphite fraction are shown in Fig. 7. A better oxygen transport and higher cathode potentials are also evidenced by the fact that in spite of the higher voltage loss at the membrane, the total electrolysis voltage, up to a current density of 400 A m^{-2}, was lower than during electrolysis employing the Bären diaphragm.

The effect of the electrode thickness on the current efficiency and electrolysis voltage was also examined. The peroxide yield was found to decrease with the thick-

ness of the 0·18–0·40 mm carbon-graphite electrode increasing over the region of 2·3 to 5·5 mm (Fig. 8). According to our calculations, this dependence is due to the higher gas and electrolyte linear velocities in the thinner electrode, which bring about high mass transfer coefficient values, and in the region where the process is transport-controlled the electrode potential is more positive and peroxide losses by reduction are lower. In accordance with this, the effect of the electrode thickness is more marked at higher current densities, where the role of mass transport is more substantial (Fig. 8). At lower current densities, where the reduction is more kinetically controlled, a negative effect arises from the smaller surface area of the thinner electrode, bringing about a more negative electrode potential (see Fig. 9, where the potential indicated is the calculated local potential at the diaphragm[18]).

The peroxide current efficiency increases appreciably with increasing pressure in the trickle-bed electrode (Fig. 10). This is due to the increasing solubility of oxygen, owing to which the rate of peroxide formation grows (Eq. (*A*)) in conditions of both transport and kinetic control of the process involved (see Eq. (*14*) in ref.[13]).

The measurements served for a basic optimization of crushed graphite trickle-bed electrodes for the reduction of oxygen to peroxide. When using the medium-size graphite fraction (0·18–0·40 mm) and an ionex membrane, rather high peroxide

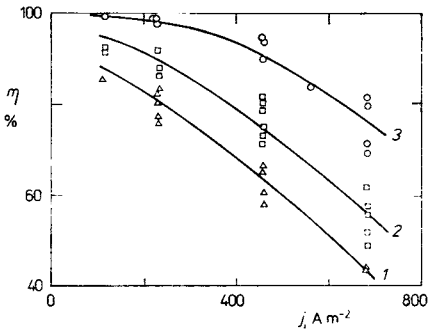

FIG. 7

Dependence of peroxide yield on current density for a carbon-graphite electrode 0·18–0·40 mm particle size. Labelling and description as in Fig. 5, Nafion 295 membrane

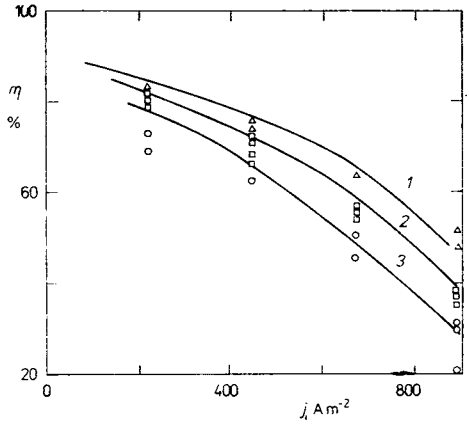

FIG. 8

Dependence of peroxide yield on current density for a carbon-graphite electrode 0·18–0·40 mm particle size, thickness (mm): *1* 2·3, *2* 3·4, *3* 5·5. Electrolyte flow rate 0·6 $dm^3\ h^{-1}$, oxygen flow rate 0·56 $dm^3 . min^{-1}$. Other labelling and description as in Fig. 5

current efficiencies (70–100% at current densities up to 0·75 kA m^{-2}) are attained also at lower pressures than have been hitherto applied[7–12]. The peroxide concentrations, however, are not very high, similarly as in other works. For instance, in measurements using an electrode containing the medium-size graphite fraction and an ionex membrane, the highest peroxide concentrations for 2M-NaOH electrolyte were 0·55 and 0·75 mol dm^{-3} at atmospheric pressure and at an overpressure of 0·5 MPa, respectively, at the electrode exit.

In comparison to gas diffusion electrodes developed for this process[5], the attained peroxide concentrations (or current efficiencies at the same peroxide concentrations) are lower. This is primarily due to a high hindrance to oxygen transport in the trickle-bed electrode caused by the limited area of the g–l interface in the electrode and the limited rate of oxygen transport through the relatively thick layer of solution trickling over the electrode material particles. As a result, the potential decreases with current density more rapidly for trickle-bed electrodes than for gas diffusion electrodes[5,18].

Ensuing work was therefore aimed at a study of trickle-bed electrodes containing, in addition to graphite, teflon-coated carbon black. By their structure, such electrodes should be a link between the hydrophilic crushed graphite trickle-bed electrodes and gas diffusion electrodes.

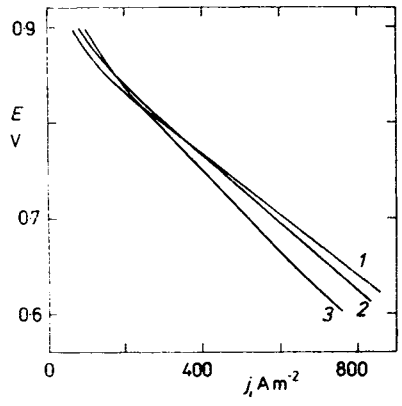

FIG. 9

Calculated polarization curves for a carbon-graphite electrode 0·18–0·40 mm particle size. Curve labelling as in Fig. 8. The values of potential are referred to the equilibrium potential of mercury–mercuric oxide electrode

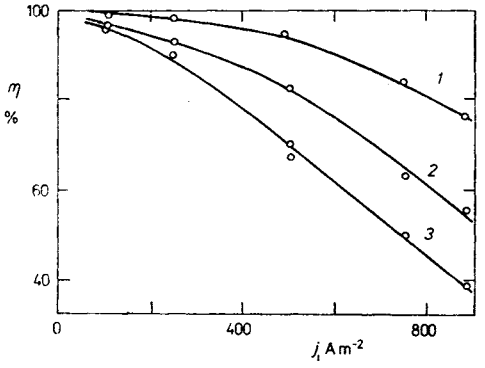

FIG. 10

Dependence of peroxide current efficiency on current density for an S 42 carbon-graphite electrode 0·18–0·40 mm particle size, separated by a Nafion 295 membrane. Electrolyte flow rate 0·6 dm^3 h^{-1}, exit oxygen overpressure (MPa): *1* 1, *2* 0·5, *3* 0. Other description as in Fig. 5

LIST OF SYMBOLS

a	electrode material surface area per unit volume in trickle-bed electrode, m^{-1}
d	spherical particle diameter, m
d'	modified particle diameter, m
$\bar{d}$	average diameter of a screened fraction, m
f_p	particle roughness factor
f_d	diaphragm pore curvature factor
Ga	modified Galileo number
j	current density, A m^{-2}
l	electrode length, m
P_d	diaphragm permeability, m^2
ΔP_G, ΔP_L	single-phase pressure loss in electrode, Pa m^{-1}
ΔP_{GL}	two-phase pressure loss, Pa m^{-1}
Re_G, Re_L	Reynolds number for gas or liquid flow in electrode
t	electrode thickness, m
t_d	diaphragm thickness, m
U_G	linear gas velocity in electrode, m s^{-1}
V_d	diaphragm porosity
w	electrode breadth, m
β_l	temporary liquid holdup in electrode
η	current efficiency of peroxide formation, %
ε	electrode porosity
μ_G	dynamic viscosity of gas, kg m^{-1} s^{-1}

REFERENCES

1. Berl E.: Trans. Electrochem. Soc. *76*, 359 (1939).
2. Ignatenko E. Kh., Barmashenko I. B.: Zh. Prikl. Khim. *17*, 2415 (1964).
3. Kastening B., Faul W.: Chem.-Ing.-Tech. MS 537/77 (1977).
4. Špalek O., Balej J.: Collect. Czech. Chem. Commun *42*, 952 (1977), *46*, 2052 (1981).
5. Špalek O., Balogh K., Balej J.: Chem. Prum. *32*, 572 (1982).
6. Špalek O., Balogh K., Paseka I.: Czech. 229 477 (1986).
7. Oloman C., Watkinson A. P.: Can. J. Chem. Eng. *54*, 312 (1976).
8. Oloman C., Watkinson A. P.: J. Appl. Electrochem. *9*, 117 (1979).
9. Oloman C., Watkinson A. P.: Sven. Papperstidn. *83*, 405 (1980).
10. McIntyre J. A., Phillips R. F.: *Meeting Electrochem. Soc., Montreal 1982;* Abstr. No 399.
11. Davison J. B., Kacsir J. M., Peerce-Landers P. J., Jasinski R.: J. Electrochem. Soc. *130*, 1497 (1983).
12. Sudoh M., Kitaguchi H., Koide K.: J. Chem. Eng. Jpn. *18*, 409 (1985).
13. Špalek O.: Collect. Czech. Chem. Commun. *51*, 1883 (1986).
14. Špalek O., Balogh K., Paseka I.: *37th Meeting of International Society of Electrochemistry*, Ext. Abstr. Vol. IKV, p. 09—40 (I). Viniti, Vilnius 1986.
15. Ergun S.: Chem. Eng. Prog. *48*, 89 (1952).
16. Sato Y., Hirose T., Takahashi I., Toda M.: J. Chem. Eng. Jpn. *6*, 147 (1973).
17. Specchia V., Baldi G.: Chem. Eng. Sci. *32*, 515 (1977).

Translated by P. Adámek.